Eur. Phys. J. C 5, 641–650 (1998)
DOI 10.1007/s100529800985

THE EUROPEAN PHYSICAL JOURNAL C

Fragmentation and particle production in interactions of 10.6 GeV/N gold nuclei with hydrogen, light and heavy targets

M.L. Cherry[2], A. Dąbrowska[1], P. Deines-Jones[2,a], R. Hołyński[1], B.S. Nilsen[2,b], A. Olszewski[1], M. Szarska[1], A. Trzupek[1], C.J. Waddington[3], J.P. Wefel[2], B. Wilczyńska[1], H. Wilczyński[1], W. Wolter[1], B. Wosiek[1], K. Woźniak[1]

[1] Institute of Nuclear Physics, Kawiory 26A, 30-055 Kraków, Poland
[2] Department of Physics and Astronomy, Louisiana State University, Baton Rouge, LA 70803, USA
[3] School of Physics and Astronomy, University of Minnesota, Minneapolis, MN 55455, USA

Received: 22 April 1998 / Published online: 8 September 1998

Abstract. We have investigated the interactions of 10.6 GeV/n Au in nuclear emulsion. Two methods of separating interactions into those with hydrogen, light (C,N,O)and heavy (Ag,Br) target nuclei were used, giving almost identical results, which strengthened our confidence in the correctness of these methods. We also measured the angular distributions of singly and multiply charged relativistic particles emitted from the interaction vertices and the charges of the multiply charged projectile fragments. The fragmentation of the projectile Au nuclei and of the target nuclei were analyzed. The multiparticle production was studied as a function of the mass of the target nucleus. The multiplicity and the pseudorapidity distributions of relativistic singly charged particles were compared with the predictions of the RQMD Model.

1 Introduction

For many years the nuclear emulsion technique has been used to investigate hadron-nucleus and nucleus-nucleus interactions. Nuclear emulsion detectors have some unique advantages, e.g. 4π detection, submicron resolution, excellent detections of both relativistic and very low energy particles, and last but not least, simplicity and relatively low costs in comparison with other techniques. One of the main disadvantages is the composite nature of the target which basically consists of three groups of nuclei: hydrogen, light (carbon, nitrogen, oxygen) and heavy (bromine, silver). Due to the large difference in mass of the projectile (gold) and any of the emulsion target nuclei it became possible in this experiment to separate from a minimum bias sample of Au interactions subsamples of interactions with the three main groups of target nuclei. This separation of Au-Em interactions allowed us to make simultaneous analysis of fragmentation processes of both the projectile and the target nuclei as well as studying the production processes as a function of the target mass, taking full advantage of the nuclear emulsion technique.

The interactions analyzed in this study include those used in a previous analysis [1] together with the enhanced sample of interactions with hydrogen target selected from the additional scanning for Au-Em interactions. This new analysis is now able to separate the interactions into three classes of target nuclei, whereas before interactions with light and hydrogen targets were not separated. In addition, in the earlier study of the gold nuclei there was no consideration of the singly charged particle multiplicities and pseudorapidity distributions, which can be compared with model predictions.

2 Experimental

Stacks composed of BR-2 nuclear emulsion pellicles with dimensions of $5\times10\,\mathrm{cm}^2$ and 0.6 mm thick were exposed to the 10.6 GeV/n gold beams at Brookhaven National Laboratory [1–3]. The stacks were oriented so that the beams were parallel to the pellicles. Interactions were found by microscope scanning along the primary tracks in order to obtain a sample with minimum detection bias. The experimentally found interaction mean free path 4.67 ± 0.10 cm [3] is in reasonable agreement with the value 4.43 cm calculated using the predicted charge changing cross sections [4] and the composition of the emulsion [5]. This value differs from that of 4.25 ± 0.1 cm calculated previously [3], due to the use of more recent evaluations of the relevant cross sections. Consequently, we can assume that there was a high efficiency of detecting the interactions, although we cannot exclude a possible minor inefficiency during the scanning, which would represent a bias against the least disruptive interactions. Our minimum bias sample consists of 1089 Au interactions in emulsion enhanced by 249 additionally analyzed Au-H interactions selected from the second scanning for Au-Em interactions. In each event analyzed, we measured the emission angles of all fast singly

[a] now at NASA Goddard Space Flight Center, Greenbelt, MD 20771, USA
[b] now at Ohio State University, Columbus, OH 43210, USA

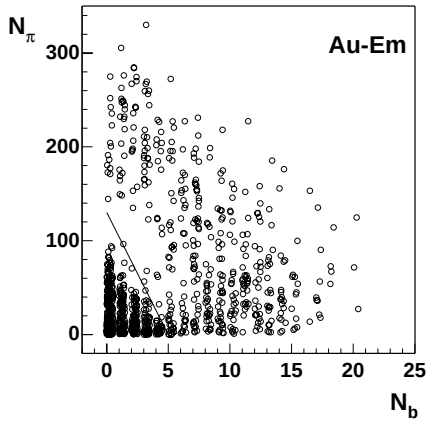

Fig. 1. The number N_π of charged particles produced vs. the number N_b of target fragments for 1089 Au-Em interactions. For explanation of the straight line see the text

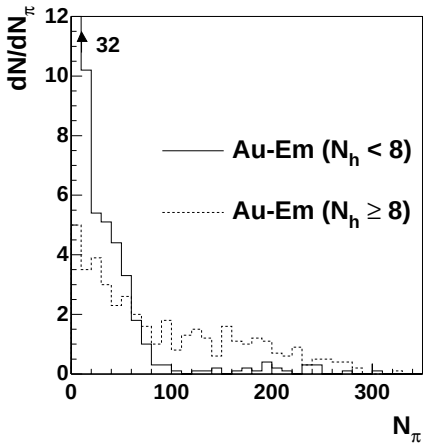

Fig. 2. The distribution of charged particles N_π produced in Au-Em interactions with heavily ionizing tracks $N_h < 8$ (solid histogram) and $N_h \geq 8$ (dashed histogram)

charged particles, helium and heavier ($Z > 2$) projectile fragments. Their numbers are denoted by N_s, N_α and N_f respectively. The charges, Z_f, of multiply charged projectile fragments were also measured [1,2] with an uncertainty not exceeding 5%. We determined the number N_g (gray tracks) of relatively slow single charged particles from the target nuclei being mostly recoil protons as well as the number N_b (black tracks) of very slow singly and multiply charged target fragments. The number of black and gray tracks are often combined into a single group of slow ($\beta < 0.7$) heavily ionizing ($I > 1.4I_o$) particles whose number is denoted by N_h, where I_o is the minimum ionization produced by relativistic singly charged particles. The separation between black and gray tracks corresponds to the ionization of a 30 MeV proton. The number of produced charged particles $N_\pi = N_s - (Z_p - Z_b)$, where Z_p is the charge of the projectile and Z_b the total charge bounded in multiply charged projectile fragments.

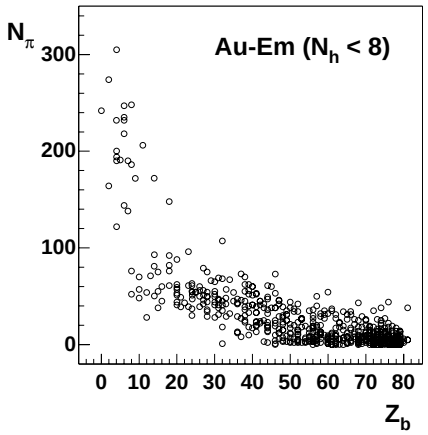

Fig. 3. The number N_π of produced charged particles vs. the total charge Z_b bounded in multiply charged projectile fragments in Au-Em interactions with $N_h < 8$

3 Separation of Au interactions with the different target nuclei in nuclear emulsion

A two step method was used to select from the minimum bias sample of interactions those with heavy, light and hydrogen targets. In the first step we identified the Au-(Ag,Br) interactions and in the next the Au-H interactions, leaving the sample of Au-(C,N,O) interactions. Two slightly different methods were used to select the Au-(Ag,Br) interactions. The first, which has been described previously [1] and used on a smaller sample, was based on a study of a scatter plot of N_π vs. N_b for the total sample of interactions. The same procedure was applied here and the corresponding plot is presented in Fig. 1.

The visible gap between the two distributions was parametrized by the same straight line as in [1], $N_\pi = 130 - 26N_b$. This line is drawn in Fig. 1. We can assume that it divides the minimum bias sample of Au-Em interactions into those with (H,C,N,O) nuclei for which $N_\pi < 130 - 26N_b$ and with (Ag,Br) nuclei for which $N_\pi \geq 130 - 26N_b$. It is natural to assume that for Au interactions with just one type of nucleus there would not be a gap on an N_π vs. N_b scatter plot, such as that seen in Fig. 1. The observed gap, which can hardly be a statistical fluctuation, must be due to Au interactions with separate groups of target nuclei of very different mass. We have made no effort to change the parametrization of the straight line plotted in Fig. 1 in order to obtain better agreement with the larger sample studied here, because in the analysis which follows we will use a slightly different selection method which appears to be less arbitrary, but gives quite consistent results.

In this second selection method we begin with a separation of interactions based on the number N_h of target fragments plus recoil protons emitted from the struck target nucleus. We assume that all events with $N_h \geq 8$ are due to Au-(Ag,Br) interactions. Among events with $N_h < 8$ are all interactions with (H,C,N,O) targets together with some admixture of Au-(Ag,Br) interactions. Figure 2 shows the N_π distributions of events for two different intervals of N_h particles. The distribution of events with $N_h < 8$ has a break at around $N_\pi = 100$, which is

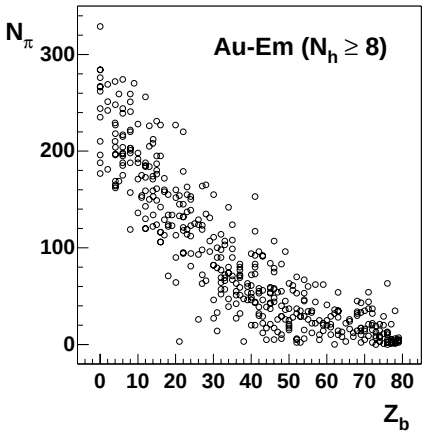

Fig. 4. The same as Fig. 3 but for Au-Em interactions with $N_h \geq 8$

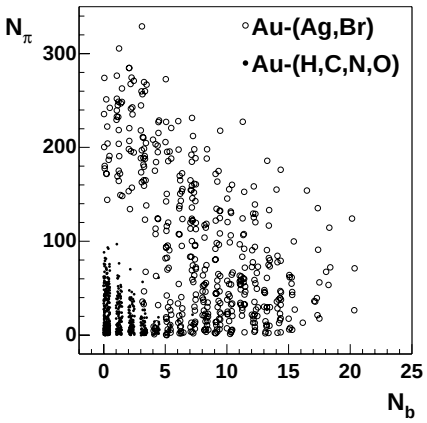

Fig. 5. Scatter plot of N_π vs. N_b for Au-(Ag,Br) and Au-(H,C,N,O) interactions

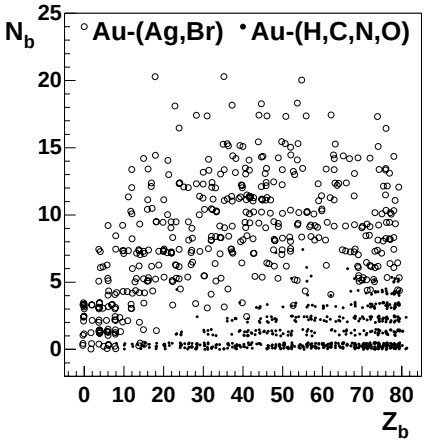

Fig. 6. Scatter plot of N_b vs. the total charge Z_b bounded in multiply charged projectile fragments in Au-(Ag,Br) and Au-(H,C,N,O) interactions

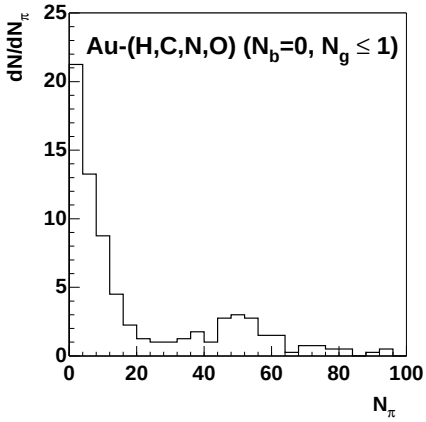

Fig. 7. The distribution of charged particles N_π produced in Au-Em interactions with $N_b = 0$ and $N_g \leq 1$

not present in the multiplicity distribution of events with $N_h \geq 8$. A smooth N_π distribution of events with $N_h \geq 8$ confirms that this sample is uniform, while the break in the N_π distribution for $N_h < 8$ is a reflection of the composite target within this sample. High multiplicity ($N_\pi \geq 100$) events are due to Au-(Ag,Br) interactions whatever their N_h. That events with $N_h < 8$ and $N_\pi \geq 100$ are separated from the rest of the $N_h < 8$ events is confirmed by the discontinuity in the relation between N_π and the total charge bounded Z_b shown in Fig. 3, whereas Fig. 4 shows that events characterized by $N_h \geq 8$ do not exhibit such a discontinuity. Figure 5 and Fig. 6 show the correlations between N_π vs. N_b and N_b vs. Z_b for the samples of Au-(Ag,Br) and Au-(H,C,N,O) interactions separated by this second method. From these plots we can see that there is a minimal overlap between the two groups and clearly that there are sparsely populated regions between the samples of interactions with different targets, confirming the efficiency and consistency of the two separation methods.

In order to extract the Au-H interactions we followed the procedure described in [6]. This we have done on the enhanced statistics obtained from the additional scanning for interactions of Au in emulsion. From the events found we selected and measured interactions with hydrogen targets using the following criteria. We assumed that in Au-H interactions there should be no fragments of the target and at most just one recoil proton may be visible (N_b=0, $N_g \leq 1$). Figure 7 shows the multiplicity distribution of produced charged particles N_π for those interactions that fulfill the above criteria. A two component structure is seen, which can be attributed to interactions with hydrogen and (C,N,O) targets. We introduced an additional criterion on the multiplicity $N_\pi \leq 23$ for Au-H interactions, and assume that events with higher multiplicities are Au-(C,N,O) interactions.

Applying these criteria to our Au-Em interactions we obtained the samples of Au interactions with hydrogen and a fraction of interactions with (C,N,O) targets. In Table 1 the number of interactions with different targets are presented and denoted as "selection 1" and "selection 2". "Selection 1" refers to the method based on the N_b vs. N_π scatter plot and "selection 2" on the N_h and N_π parameters. The number of Au-H interactions does not depend on the separation methods used for Au-(Ag,Br) interactions.

It is true that both separation methods of Au-(Ag,Br) interactions may introduce small biases. For instance it is

Table 1. Parameters describing Au interactions with different targets. For explanation see the text

	Au-Em	Au-Ag,Br selection		Au-C,N,O selection		Au-H	
		1	2	1	2		
N	1089	469	451	415	433	454[a]	205[b]
%exp.	100	43±2	41±2	38±2	40±2		19 ±2
%calc.	100	45		36			19
$\langle N_\pi \rangle$	50.3±2.0	92.0± 3.7	95.1± 3.7	25.1± 1.1	24.5± 1.0	5.7± 0.2	
$\langle N_a \rangle$	4.34± 0.09	4.5± 0.1	4.54± 0.14	4.5± 0.2	4.45± 0.16	3.56± 0.13	
$\langle N_f \rangle$	1.91± 0.04	1.74± 0.06	1.74± 0.07	2.10± 0.07	2.09± 0.06	1.91± 0.06	
$\langle N_{\alpha+f} \rangle$	6.3± 0.1	6.2± 0.2	6.3± 0.2	6.6± 0.2	6.5± 0.2	5.5± 0.2	
$\langle Z_f \rangle$	21.3± 0.5	16.4± 0.7	15.8± 0.7	21.3± 0.8	21.7± 0.8	31.5± 0.9	
$\langle Z_b \rangle$	49.4± 0.7	37.6± 1.1	36.6± 1.1	53.8± 1.0	54.2± 1.0	67.1± 0.5	
$\langle N_b \rangle$	3.92± 0.14	7.9± 0.2	7.98± 0.20	1.37± 0.06	1.53± 0.07	0	
$\langle N_g \rangle$	4.35± 0.15	8.8± 0.2	9.08± 0.22	1.44± 0.06	1.43± 0.06	0.11± 0.01	
$\langle N_h \rangle$	8.27± 0.26	16.7± 0.3	17.1± 0.3	2.82± 0.09	2.97± 0.09	0.11± 0.01	

[a] The enhanced sample of interactions from the additional scanning
[b] The sample selected from 1089 inclusive Au-Em interactions

not possible to distinguish very peripheral Au interactions with (Ag,Br) targets characterized by $N_h < 8$ and small N_π from Au interactions with (H,C,N,O). That these biases are small is shown by a comparison of the experimentally obtained percentages of interactions with hydrogen, light and heavy nuclei of emulsion and those calculated from the predicted nucleus-nucleus charge changing cross sections [4] and the composition of emulsion [5] (see Table 1). Taking into account the uncertainties in evaluations of the charge changing cross sections, which can be as high as 10%, there is a satisfactory agreement between the experimental and the calculated fractions for each type of target nuclei.

4 Fragmentation of the projectile gold nucleus

In Fig. 8 we present the charge Z_f distributions of multiply charged projectile fragments with $Z > 2$ emitted from Au-Em, Au-H, Au-(C,N,O) and Au-(Ag,Br) interactions. Their mean values $\langle Z_f \rangle$ are given in Table 1. The lighter the target nucleus, the more frequent are heavier projectile fragments. As a consequence, one observes an increase of $\langle Z_f \rangle$ with decreasing mass of the target nucleus (see Table 1). However, even for the hydrogen target the light projectile fragments are the most frequent. Fragments with charges around half of the primary charge are the rarest ones irrespective of the mass of the target nucleus. This is partially a consequence of the fact that fission in this sample of Au-Em interactions is very rare [7].

The distribution of the number of multiply charged fragments $N_{\alpha+f}$ for light (C,N,O) and heavy (Ag,Br) target nuclei are similar but differ appreciably from that produced by a hydrogen target (see Fig. 9). All interactions produce some alpha or heavier fragments, while only

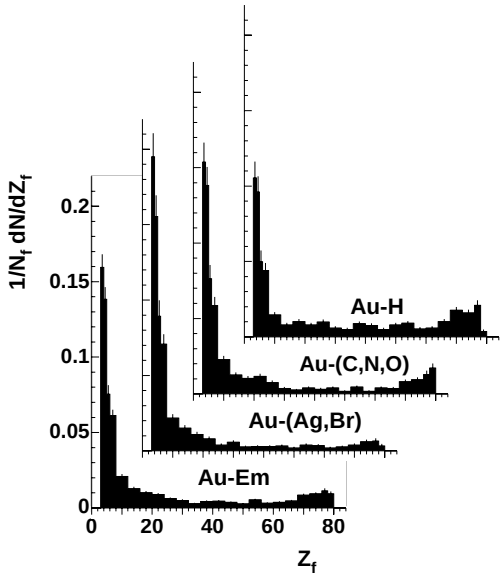

Fig. 8. Charge distributions of multiply charged projectile fragments ($Z_f > 2$) in Au interactions with emulsion, (Ag,Br), (C,N,O) and hydrogen target (scales are the same for all distributions)

those interactions with heavy targets can have no multiply charged projectile fragments. Figure 10 and Fig. 11 show the distribution of N_α and N_f. For a hydrogen target the most frequent events are those with one alpha fragment and one heavier fragment. The mean number of helium fragments emitted in interactions with hydrogen is smaller than in collisions with heavier targets (see Table 1). For a hydrogen target there are no events with $N_f = 0$, while 50% of events have only one fragment with $Z > 2$. For heavier targets, the fraction of events with $N_f = 0$ increases while the fraction of events with $N_f = 1$ decreases with increasing target mass. The probability of interac-

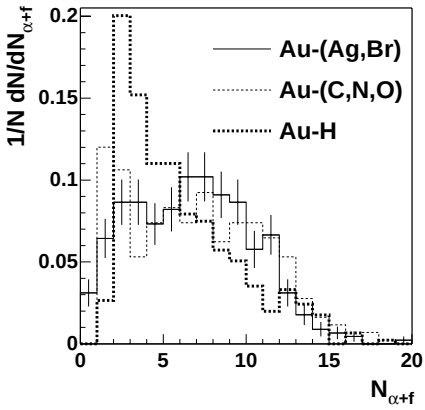

Fig. 9. Frequency distributions of numbers of multiply charged projectile fragments $N_{\alpha+f}$ in Au interactions with (Ag,Br), (C,N,O) and hydrogen targets

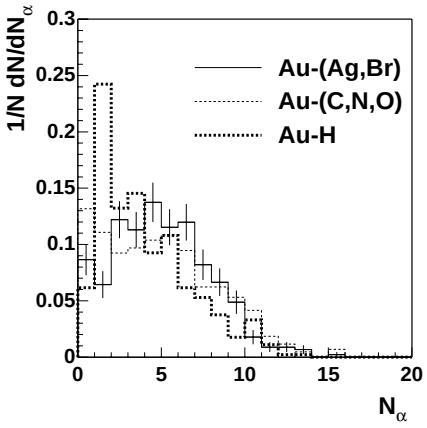

Fig. 10. Frequency distributions of the number of helium fragments N_a in Au interactions with (Ag,Br), (C,N,O) and hydrogen targets

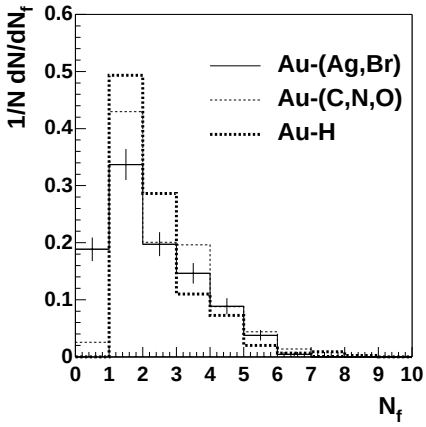

Fig. 11. Frequency distributions of the number of projectile fragments N_f with the charge $Z > 2$ in Au interactions with (Ag,Br), (C,N,O) and hydrogen targets

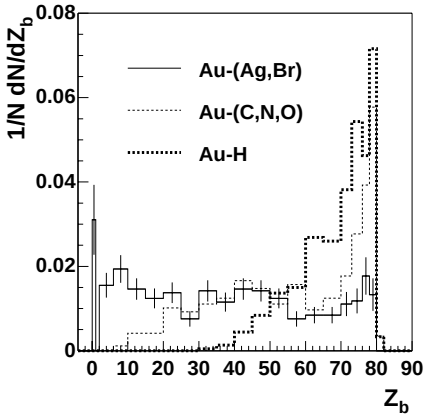

Fig. 12. The distribution of the total charge Z_b bounded in multiply charged projectile fragments in Au interactions with (Ag,Br), (C,N,O) and hydrogen targets

Table 2. The probability of Au interactions with different number N_f of fragments with $Z > 2$ as a function of the mass of the target

Target	number of fragments		
	0	1	>1
H	0	0.49±0.03	0.51±0.03
C,N,O	0.02±0.01	0.43±0.03	0.54±0.04
Ag,Br	0.19±0.02	0.34±0.03	0.47±0.03

tions heaving different numbers of fragments N_f depends on the mass of the target. For $N_f = 0$ the probability increases with the target mass; it decreases for $N_f = 1$; and for $N_f > 1$ i.e. for multifragmentation [3] it becomes independent of the mass of the target (see Table 2).

The probability distributions of the total charge Z_b remaining in multiply charged projectile fragments in interactions with different targets are shown in Fig. 12. These distributions depend strongly on the mass of the target. For hydrogen targets the Z_b distribution is peaked close to the charge Z_p of the primary, and essentially does not extend below $Z_p/2$ while for (Ag,Br) targets the distribution is almost flat over the entire Z_b range. This behavior results in the decrease in $\langle Z_b \rangle$ with increasing mass of the target (see Table 1).

The differences in the fragmentation of the projectile nucleus on various targets are apparent. An alternative method of presenting them can be seen on the plots, Fig. 13, that show the relation between $(Q_F - Z_1)$ and Z_1, where Q_F stands for the total charge emitted in the very forward direction and Z_1 is the charge of the heaviest fragment of the Au projectile. The Q_F value includes the charges of all multiply charged projectile fragments plus a number of singly charged relativistic particles with pseudorapidities $\eta = -ln\ tan(\theta/2) > 3.6$. This η value was obtained from the relation: $6.5 - ln(200/10.6) = 3.6$ where $\eta = 6.5(\theta = 3mrad)$ represents the half opening cone, for oxygen and sulfur interactions at 200 GeV/n, in which almost all spectator protons were contained and the number of produced particles was small. This angle was verified [8] using the VENUS Model [9] calculations. The second term in the above relation is the factor by which the Au energy 10.6 GeV/n has to be boosted to be matched with the

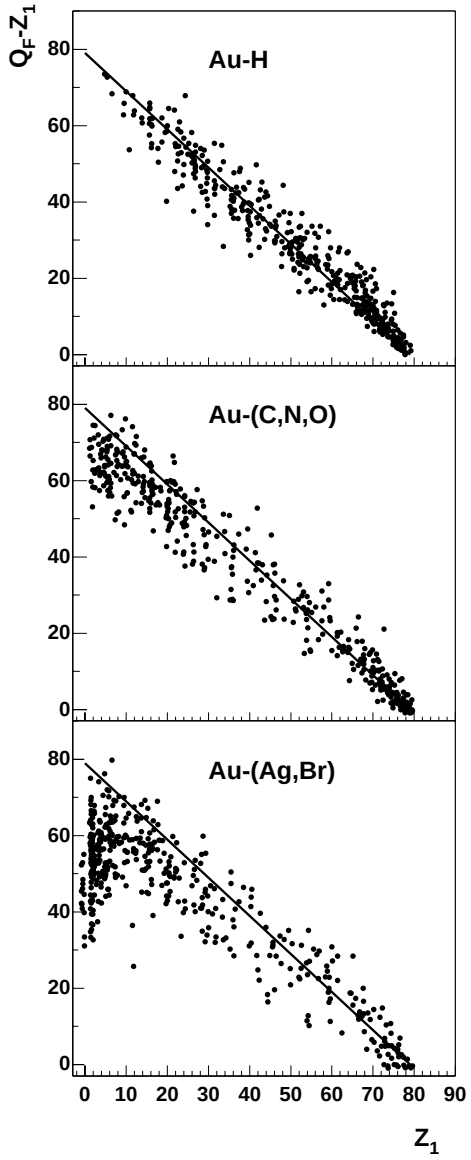

Fig. 13. Scatter plots between $(Q_F - Z_1)$ and Z_1 for Au interactions with (Ag,Br), (C,N,O) and hydrogen. See the text for explanation

data at 200 GeV/n. Figure 13 shows the $(Q_F - Z_1)$ vs. Z_1 for the three classes of targets. In general, the observed events follow the straight line $Z_1 + (Q_F - Z_1) = Z_p$ where Z_p is the charge of the projectile nucleus. This means that in the majority of interactions (at least with light targets) the Q_F value does not differ very much from the charge of the primary. This is what is seen for the hydrogen target, suggesting that the number of intranuclear nucleon-nucleon inelastic collisions is small. It appears that events scatter along this line. This is either due to the inclusion of produced particles emitted at small angles into Q_F or to the exclusion from Q_F of protons scattered at large angles. An additional deviation from this line can also be due to the uncertainties in the charge determination of the projectile fragments. Among the events characterized by small value of Z_1 and representing interactions with

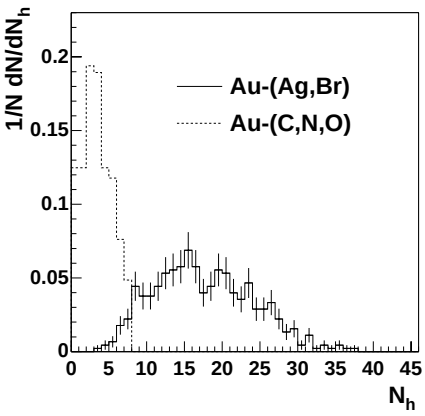

Fig. 14. The distributions of the number N_h of target fragments plus recoil protons emitted from the struck target nucleus in Au interactions with (Ag,Br) and (C,N,O) targets

targets heavier than hydrogen there is a class of events with $Q_F < Z_p$. This indicate that as the mass of the target increases, the projectile protons are scattered out of the cone, i.e. the number of intranuclear nucleon-nucleon inelastic collisions increases as the mass of the target increases.

5 Fragmentation of the target nuclei

Fragmentation of the target nucleus is manifested by the emission of slow heavily ionizing particles. Figure 14 shows the distribution of the number N_h of target fragments plus recoil protons in Au interactions with (Ag,Br) and (C,N,O) nuclei. The N_h distribution in interactions of Au in emulsion is shown in Fig. 15. The visible three component structure of the N_h distribution reflects Au interactions with the three groups of target nuclei present in nuclear emulsion. Similar structure in the N_h distribution is also seen in sulfur and oxygen interactions at 200 GeV/n [8,10,11] and even in proton-emulsion interactions at 200 GeV (see Fig. 15). The mean number of N_h in interactions of Au, S, O and proton with nuclear emulsion is equal to 8.3±0.3, 8.1±0.3, 8.5±0.3 and 7.6±0.2 respectively. We can calculate the expected $\langle N_h \rangle$ in Au-Em interactions by using the charge changing cross sections [4], composition of emulsion [5] and the experimentally found average N_h numbers for the Au interactions with the three different targets in emulsion. We obtain $\langle N_h(Au, Em) \rangle = \sum P(A_t) \langle N_h(A_t) \rangle = 8.7$, where $P(A_t)$ is the frequency of Au interactions with a target of mass A_t for which the mean number of heavily ionizing particles is $\langle N_h(A_t) \rangle$. Within the uncertainties, which can be as high as 10% the number $\langle N_h \rangle = 8.7$ is in agreement with 8.3 ± 0.3. This provides further support for the validity of the selection method used to separate Au interactions with the various emulsion targets.

The fact that the $\langle N_h \rangle$ values in interactions of S and O with emulsion are the same as the $\langle N_h \rangle$ value for Au-Em interactions does not necessarily mean that for a given target the $\langle N_h \rangle$ is the same irrespective of the mass and/or

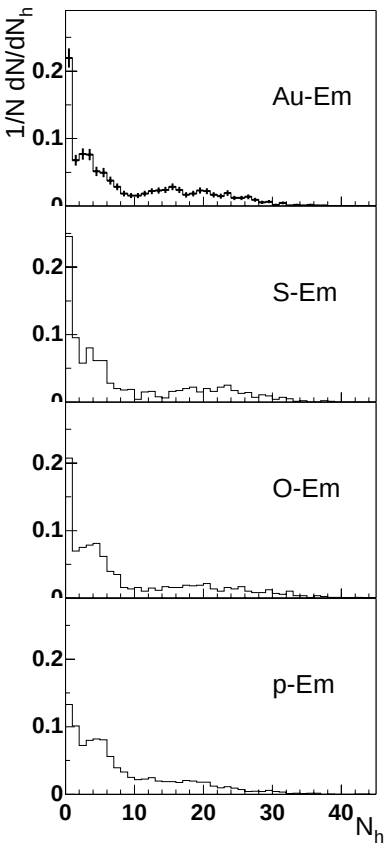

Fig. 15. The distributions of the number N_h of target fragments plus recoil protons in interactions of Au, S, O and p in emulsion

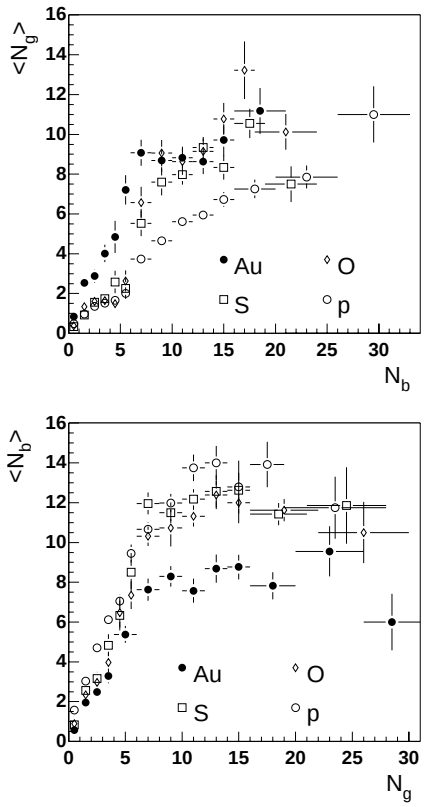

Fig. 16. The dependencies of the mean number $\langle N_g \rangle$ of recoil protons on the number N_b of target fragments and $\langle N_b \rangle$ on N_g in interactions of Au, S, O and p in emulsion

energy of the projectile. The relative contributions with hydrogen, light and heavy emulsion targets to the total number of inclusive interactions in emulsion depends on the mass of the projectile nucleus. Assuming the same numbers of $\langle N_h \rangle$ for O and S interactions with hydrogen, (C,N,O) and (Ag,Br) targets as for the Au projectile, and calculating contributions from different targets to the total number of interactions in emulsion, we get predicted values for $\langle N_h \rangle$ of 10.3 and 10.8 for S and O interactions in emulsion, instead of the observed values 8.1 ± 0.3 and 8.5 ± 0.3. Apparently, for a given target, $\langle N_h \rangle$ must be a function of the mass of the projectile. For an (Ag,Br) target and Au projectiles $\langle N_h \rangle = 17.1 \pm 0.3$ (see Table 1). For S and O projectiles this number must be smaller in order to achieve $\langle N_h \rangle \simeq 8$ in emulsion, instead of the calculated value of about 10. This difference is more drastic for proton interactions in emulsion. Under the assumption that for proton projectiles $\langle N_h \rangle$ for H, (C,N,O) and (Ag,Br) targets are the same as those for an Au projectile, the calculated $\langle N_h \rangle$ for proton-emulsion interactions equals about 13 in comparison with the experimental $\langle N_h \rangle = 7.6 \pm 0.2$. Since these energies are well above the threshold for limiting fragmentation [12] it may be concluded that the N_h distributions do depend on the mass of the projectile.

The dependencies of the mean numbers of recoil protons (gray tracks) $\langle N_g \rangle$ on the number of target fragments (black tracks) N_b and the $\langle N_b \rangle$ on N_g in Au-Em interactions are shown in Fig. 16. We observe an increase of $\langle N_g \rangle$ with increasing N_b and an increase of $\langle N_b \rangle$ with increasing N_g, then an apparent leveling for the values of N_b and N_g greater than about 8. Similar correlations exist in sulfur, oxygen and proton interactions in emulsion at 200 GeV/n (see Fig. 16). For primary protons an increase of $\langle N_g \rangle$ with increasing N_b continues up to the highest values of N_b. For heavier projectiles (Au) the $\langle N_g \rangle$ increases faster and the mean number $\langle N_b \rangle$ saturates at a smaller value of N_b than it does for the interactions of light and more energetic projectiles.

In Fig. 17 we present the dependencies of $\langle N_g \rangle$ on N_b and vice versa for interactions of Au with (C,N,O) and (Ag,Br) targets. It is seen that for Au-(Ag,Br) interactions there is essentially no dependence of $\langle N_g \rangle$ on N_b and $\langle N_b \rangle$ on N_g along the entire range of N_b and N_g variables and only a weak correlation for Au-(C,N,O) interactions for the small and large values of N_b or N_g. For interactions with (C,N,O) the decrease of the mean numbers of $\langle N_g \rangle$ and $\langle N_b \rangle$ at large values of N_g or N_b is a consequence of the constraint $N_h < 8$. From the above considerations it follows that the observed correlation between the N_b and N_g variables in Au-Em interactions (see Fig. 16) must be due to the composite target. The lack of dependencies between the N_b and N_g variables observed in particular in Au interactions with the heavy targets can be interpreted as an indication that the excitation of the target nucleus

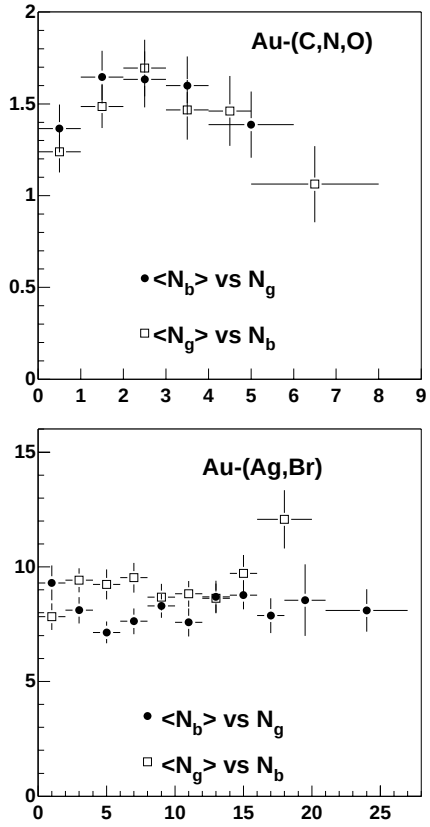

Fig. 17. The dependencies of the mean number $\langle N_g \rangle$ of recoil protons on the number N_b of target fragments and $\langle N_b \rangle$ on N_g in interactions of Au with (Ag,Br) and (C,N,O) targets

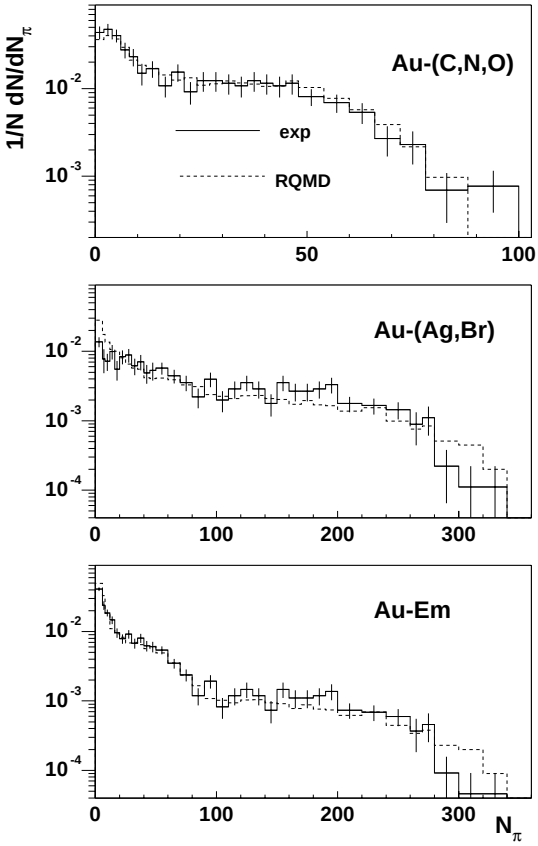

Fig. 18. Multiplicity distributions of produced charged particles in interactions of Au with emulsion, (Ag,Br) and (C,N,O) targets in comparison with the RQMD calculations

which is manifested by the emission of heavily ionizing particles is limited [13]. Assuming that the parameterN_g is a measure of the number of intranuclear collisions [14], it is astonishing that this limit is already attained at a small values of N_g, i.e. at quite large values of the impact parameter.

6 Particle production

6.1 Multiplicity distribution

The multiplicity distributions of particles N_π produced in Au interactions with (C,N,O), (Ag,Br) and emulsion are shown in Fig. 18. As was mentioned in Sect. 3, some biases against low multiplicity events could occur during scanning. In addition, some low multiplicity Au-(Ag,Br) interactions could be misclassified as Au-(C,N,O). Also, the uncertainty in charge determination of very heavy multiply charged projectile fragments of about 5% introduces some uncertainties in determination of N_π in small multiplicity events. Such events are the most abundant of the Au-H interactions. For these reasons Fig. 18 does not show the multiplicity distributions of Au interactions with hydrogen. Note that even for the heaviest target (Ag,Br) the low multiplicity events are most frequent. Also in Fig. 18 we plot the multiplicity distributions of produced charged particles predicted by the Relativistic Quantum Molecular Dynamics (RQMD) Model (version 2.2) [15]. This is the Monte Carlo model which can be used for comparison with interactions of such relatively low energy. A sample of 10,000 events was generated. The number of simulated Au interactions with the particular targets was calculated using the charge changing cross sections [4] and the composition of emulsion [5]. Figure 18 uses a semilogarithmic plot in order to emphasize the comparison at large multiplicities. In Table 3 the mean numbers of produced charged particles in Au interactions for hydrogen, (C,N,O), (Ag,Br) and emulsion are compared with the RQMD Model predictions. There is a good agreement between the Au-(C,N,O) data and the RQMD Model predictions and some discrepancies in Au-(Ag,Br) interactions. They exist in the total sample of Au-Em interactions and therefore cannot be due to an incorrect separation of events. Scanning inefficiencies in these high multiplicity events are not expected to occur. Thus, the disagreement indicates a problem with the RQMD Model. Aside from the discrepancy of Au-(Ag,Br) we can conclude that the RQMD Model reproduces the experimental shapes of the multiplicity distributions with fair accuracy.

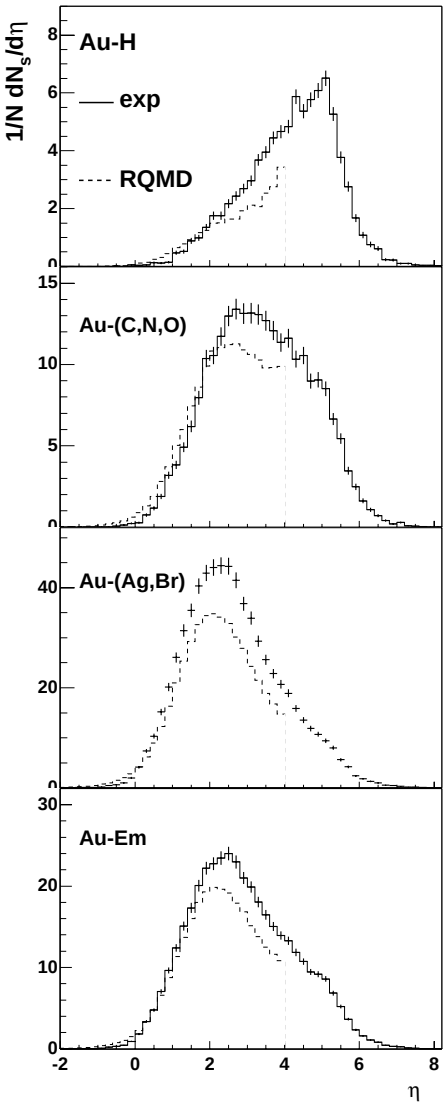

Fig. 19. Psuedorapidity distributions of singly charged relativistic particles N_s emitted from Au interactions with different targets and the RQMD Model predictions (dashed line)

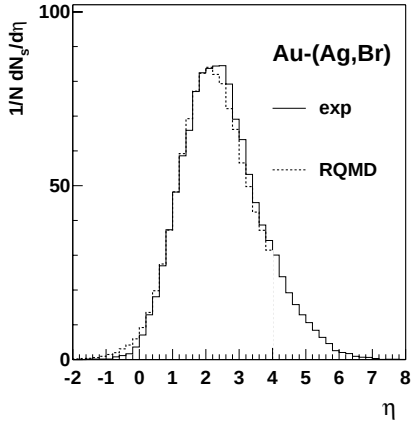

Fig. 20. Pseudorapidity distributions of singly charged relativistic particles N_s emitted from central ($N_\pi \geq 100$) collisions of Au with (Ag,Br) targets and the RQMD Model predictions

Table 3. The mean number N_π of produced charged particles of Au interactions with different targets

	Au-Em	Au-Ag,Br	Au-C,N,O	Au-H
Experiment	50.3±2.0	95.1±3.7	24.5±1.0	5.7±0.2
RQMD	45.5±0.6	78.8±1.2	25.7±0.4	4.4±0.1

6.2 Pseudorapidity distribution of singly charged particles

Figure 19 presents the pseudorapidity distributions for the singly charged relativistic particles emitted from interactions of Au with hydrogen, (C,N,O), (Ag,Br) and emulsion. These distributions are asymmetric with respect to $\eta = (1/2)ln(2E/M) = 1.6$, the rapidity corresponding to 90 degrees in p-p CM system. The smaller the mass of the target nucleus, the more asymmetric is the pseudorapidity distribution. The observed forward asymmetry follows from three sources: the asymmetry of the colliding nuclei (the projectile nucleus is always more massive than the heaviest target nucleus), the presence of released projectile protons which are emitted forward and the difference between the measured pseudorapidity and the rapidity. In Fig. 19 we also plotted the pseudorapidity distributions of singly charged relativistic particles predicted by the RQMD Model. A comparison is restricted to $\eta < 4$. Above this η value there are also multiply charged projectile fragments, whereas in RQMD simulations the multiply charged projectile fragments are always resolved into protons. A comparison for $\eta > 4$ is therefore meaningless. In general, the experimental distributions for the η values greater than about 2 are higher than those predicted by the RQMD Model and the peak positions are shifted towards higher values of η than those predicted by the RQMD Model. However, it is worthwhile to notice that there is an excellent agreement between the predictions of the RQMD Model (also restricted to the η values less than 4) and the central collisions of Au projectiles with heavy (Ag,Br) targets. This comparison is shown in Fig. 20, where the central collisions with (Ag,Br) were selected by the number of produced charged particles $N_\pi \geq 100$.

7 Conclusion and discussion

We have shown that the minimum bias sample of 10.6 GeV/n Au interactions in emulsion can be separated into samples of events with hydrogen, light (C,N,O) and heavy (Ag,Br) target nuclei. This separation is accomplished using two slightly different methods. One is based on the correlation between the number, N_π, of charged particles produced and the number N_b of fragments from target nuclei; the other on the number N_h of target fragments plus recoil protons and the cut imposed on N_π. In both methods the same procedure of extracting Au-H interactions is used. It appears that both separation methods give approximately the same results (see Table 1).

The fragmentation of the projectile gold nucleus depends on the target. This is manifested in different distributions of the charged Z_f of fragments and of the distributions of the total charge, Z_b, confined in multiply charged projectile fragments. The lighter the target nucleus, the more frequent are heavier projectile fragments and the larger the mean values of the total charge confined in multiply charged projectile fragments.

The probability of interactions without any projectile fragments with charges $Z > 2$ is zero for a hydrogen target, but increases with the increasing mass of the target. An opposite tendency is observed for events with only one fragment, while for events with more than one fragment the dependence on the mass of the target is very weak.

Since in our experiment the projectile nucleus is always much bigger than even the most massive target nucleus, the majority of interactions which occur in emulsion are peripheral from the point of view of the projectile fragmentation. This applies to nearly all interactions with hydrogen and the majority of interactions with light nuclei (see Fig. 13). Only for Au interactions with heavy (Ag,Br) nuclei the number of intranuclear collisions is large, leading to events with small charge Z_1 of the heaviest fragment of the projectile and also a small total charge, Q_F, emitted forward.

The three component structure of the distribution of heavily ionizing particles, N_h, emitted from the emulsion target nuclei is observed not only in the present sample of Au interactions, but also in interactions of lighter ions like sulfur and oxygen and even in proton interactions in emulsion. This effect has found a convincing interpretation when the separation of the three subsamples of Au interactions with hydrogen, light (C,N,O) and heavy (Ag,Br) nuclei of emulsion was done. We show that the mean number of heavily ionizing particles emitted from a given struck target nucleus increases with increasing mass of the projectile.

Another feature which follows from the analysis of target fragmentation is the observed lack of correlation between the number, N_b, of target fragments and the number, N_g, of recoil target protons, at least for gold interactions with (Ag,Br) nuclei. For lighter targets there may be a weak positive correlation between these quantities at their small values.

For Au-(Ag,Br) interactions, we do not see any dependence between the number of recoil protons and the mean number of fragments emitted from the target nucleus. Assuming that the number of fragments emitted from the struck target nucleus can be interpreted as a measure of the temperature of the residual nucleus, the data presented support our earlier statement [13] about the existence of a critical temperature of the excited target nucleus.

An attempt to describe the experimental data by the RQMD simulations is only partially satisfactory. The Au - H data are too uncertain to be compared with the predictions. This follows from the fact that the Au - H interactions are the most biased sample due to the possible scanning losses because of the low multiplicity of produced particles. As far as Au interactions with heavier targets are concerned there is a possibility that some low multiplicity Au-(Ag,Br) interactions accompanied by low excitation of the target nucleus would be misclassified as Au-(C,N,O) interactions. This might at least partially explain the insufficiency of Au-(Ag,Br) interactions and the overabundance of Au-(C,N,O) interactions in comparison with the calculated values. Another limitation which follows from the RQMD Model is the upper bound at $\eta = 4$. Above this pseudorapidity there are singly charged particles and multiply charged projectile fragments while in RQMD simulations only produced particles and protons. Therefore, the comparison of the experimental data with RQMD has to be restricted to pseudorapidities not greater than 4. The RQMD simulations differ from the experimental data on multiplicity distributions of Au-(Ag,Br) interactions. Nevertheless, the shapes of the multiplicity distributions of Au interactions with the light and heavy targets of emulsion are roughly reproduced by the RQMD Model. The same is true for the shapes of the pseudorapidity distributions (in the restricted pseudorapidity interval) and the position of the peaks of pseudorapidity distributions. The peak positions move to higher values of pseudorapidity with decreasing target mass. This is true for both the experimental and simulated data from the RQMD Model. The difference in the pseudorapidity peak positions between the RQMD simulations and the experiment does not exceed half a unit of pseudorapidity. The pseudorapidity distribution of the central collisions of Au-(Ag,Br) agrees well with the predictions of the RQMD Model.

Acknowledgements. This work was partially supported in Poland by a State Committee for Scientific Research Grant No. 2P03B18409 and by M. Skłodowska-Curie Fund II No. PAA/NSF-96-256, at Louisiana State University by grants from NSF, Nos: PHY-9513997 and INT-8913051, and at the University of Minnesota by DOE Grant No. DOE-FG02-89ER40528.

References

1. M.L. Cherry et al., Z. Phys. C **63**, 549 (1994)
2. M.L. Cherry et al., Z. Phys. C **62**, 25 (1994)
3. M.L. Cherry et al., Phys. Rev. C **52**, 2652 (1995)
4. B.S. Nilsen et al., Phys. Rev. C, 3277 (1995)
5. L.H. Bokova (private communication)
6. R. Hołyński et al., Proc. of the XXIV ICRC, Rome 1995, Vol. 3 p. 172
7. R. Hołyński, Nucl. Phys. A **566**, 191c (1994)
8. A. Dąbrowska et al., Phys. Rev. D **47**, 1751 (1993)
9. K. Werner, Preprint HD-TVP-93-91, (1993)
10. L.M. Barbier et al., Phys. Rev. Lett **60**, 405 (1988)
11. L.M. Barbier et al., Nucl. Phys. A **498**, 535c (1989)
12. A.C. Cummings, C.J. Waddington, Proceedings of April 1998 APS meeting
13. A. Dąbrowska et al., Z. Phys. C **59**, 399 (1993)
14. J.B. Anderson. Phys. Lett. **73B**, 343 (1978); M.K. Hegab, J. Hufner. Phys. Lett. **105B**, 105 (1981); Nucl. Phys. A **348**, 353 (1982)
15. H. Sorge et al., Nucl. Phys. A **498**, 567c (1989); Preprint UFTP, 243 (1990)